ANTIOXIDANTS & REDOX SIGNALING
Volume 25, Number 10, 2016

DOI: 10.1089/ars.2016.6751

Discoveries

FORUM REVIEW ARTICLE

In Vivo Detection of Reactive Oxygen Species and Redox Status in *Caenorhabditis elegans*

Bart P. Braeckman,[1] Arne Smolders,[1] Patricia Back,[1,*] and Sasha De Henau[1,2]

Abstract

Significance: Due to its large families of redox-active enzymes, genetic amenability, and complete transparency, the nematode *Caenorhabditis elegans* has the potential to become an important model for the *in vivo* study of redox biology. ***Recent Advances:*** The recent development of several genetically encoded ratiometric reactive oxygen species (ROS) and redox sensors has revolutionized the quantification and precise localization of ROS and redox signals in living organisms. Only few exploratory studies have applied these sensors in *C. elegans* and undoubtedly much remains to be discovered in this model. As a follow-up to our recent findings that the *C. elegans* somatic gonad uses superoxide and hydrogen peroxide (H_2O_2) signals to communicate with the germline, we here analyze the patterns of H_2O_2 inside the *C. elegans* germline. ***Critical Issues:*** Despite the advantages of genetically encoded ROS and redox sensors over classic chemical sensors, still several general as well as *C. elegans*-specific issues need to be addressed. The major concerns for the application of these sensors in *C. elegans* are (i) decreased vitality of some reporter strains, (ii) interference of autofluorescent compartments with the sensor signal, and (iii) the use of immobilization methods that do not influence the worm's redox physiology. ***Future Directions:*** We propose that several of the current issues may be solved by designing reporter strains carrying single copies of codon-optimized sensors. Preferably, these sensors should have their emission wavelengths in the red region, where autofluorescence is absent. Worm analysis could be optimized using four-dimensional ratiometric fluorescence microscopy of worms immobilized in microfluidic chips. *Antioxid. Redox Signal.* 25, 577–592.

Detecting Reactive Oxygen Species

REACTIVE OXYGEN SPECIES (ROS) are oxidizing agents that are formed by single electron transfers or by ionizing radiation and are involved in several biological processes, such as signaling, pathogen defense, and crosslinking of structural components. When levels exceed a certain threshold, they may cause oxidative stress and become harmful (45). Because they often have a short lifetime and very local occurrence, detecting and quantifying ROS have always been a technical challenge. However, some ROS are less reactive and hence show a longer lifetime and greater diffusibility, making detection somewhat easier.

The majority of studies apply reduced dyes, such as dihydrofluoresceins, dihydroethidines, coumarine derivatives, amplex red, MitoSOX™, and lucigenins [extensively reviewed in refs. (8, 45)]. Most of these dyes have fluorescent or luminescent properties, making them very sensitive. However, most probes suffer problems with specificity, stability, and uptake rate and can potentially create new radicals or interfere with the biological process under study [reviewed in ref. (129)]. Many of these dyes are irreversibly oxidized by ROS, which technically precludes long-term dynamic measurements. As uptake and distribution of chemical ROS probes are often variable and difficult to control in whole animals, experiments are often performed on isolated tissues, cells, or crude cell fractions. Taking into account the delicate intracellular redox balances, tests in which the biological material is perturbed may suffer oxidation artifacts (84). Some of the shortcomings of the dyes have been tackled by the introduction of protein-linked chemical ROS reporters (113) and ratiometric mass spectrometry probes (25), but these

[1]Biology Department, Ghent University, Ghent, Belgium.
[2]Biomedical Genetics, University Medical Center Untrecht, Utrecht, The Netherlands.
*Current affiliation: Bayer CropScience NV, Innovation Center—Seeds, Seed and Trait Safety, Zwijnaarde, Belgium.

techniques do not allow dynamic real-time measurements or may require specialized equipment. Recently, a new class of boronated dyes have been developed and applied in *Caenorhabditis elegans* to specifically quantify and localize hydrogen peroxide (H_2O_2) levels *in vivo* (29, 42).

A second class of ROS and redox probes are the genetically encoded sensors based on mutated green fluorescent proteins (GFPs). GFP has unique properties that make it very suitable as the template for such sensors. First, GFP is quite stable and biologically inert as it is very resistant to degradation by intracellular proteases and does not tend to interact much with other cellular processes. Second, wild-type GFP has two excitation peaks, at 395 and 475 nm, depending on the protonation of Y66 within the chromophore (20, 84), while there is only one emission peak at 509 nm. This property allows the estimation of the chemical status of GFP by ratiometric fluorimetry using both excitation wavelengths. Protonation of the GFP fluorophore depends on interactions with amino acid residues that are in close proximity. Hence, conformational changes in the GFP may cause the fluorescence, by excitation at 395 and 475 nm, to shift in opposite directions. Ratiometric fluorimetry is independent of the cellular expression level of the probe or photobleaching effects. Current ROS and redox-sensitive probes make use of this property (84), which overcomes an important weakness of many chemical probes in which photobleaching effects or differences in probe uptake rates between samples cannot be accounted for.

Unlike nonprotein-linked chemical ROS probes, genetically encoded sensors can be targeted to specific locations in the organism or in the cell. This is of crucial importance as many ROS and redox processes show highly specific spatial patterns (27, 86). By using tissue-specific promoters or subcellular localization signals, the sensor can be targeted to the desired tissue or organelle. The genetically encoded sensors can also be anchored to either side of an organelle or plasma membrane by placing them in tandem with gene fragments that encode for protein domains that are responsible for this specific localization (transmembrane domains, myristoylation, palmitoylation sequences, and so on).

While many chemical probes suffer certain degrees of nonspecificity, genetically encoded sensors may react highly specific with the redox-active component of interest as catalytic domains of existing redox enzymes can be included in the design.

Caenorhabditis elegans: A Good Model for *In Vivo* ROS and Redox Detection

The nematode *C. elegans* is an invertebrate model organism that is currently under investigation in over 1100 laboratories worldwide, and, on average, every 3–3.5 h a new study mentioning this worm is published. There are many reasons for the popularity of this nematode. Culture maintenance is easy and cheap as these worms are 1-mm bacterivores that can be maintained in large populations on simple agar plates seeded with *Escherichia coli* as a food source. The occurrence of hermaphrodites as well as males, the 3-day lifecycle, and the possibility of recovery after liquid nitrogen storage are unique features, absent in other multicellular models, which made *C. elegans* a prime genetic tool. The limited anatomical complexity and lifelong transparency of this animal greatly helped in the complete documentation of its development (118) and neuroarchitecture (130). The next milestones supported further maturation of this model into its current form: introduction of GFP as an expression reporter (19), the early completion of its genomic sequence (1), the discovery and use of RNA interference (RNAi) (120), and the development of a freely accessible online web database (114). With these (and many other) tools at hand many biological processes have been studied in unsurpassed molecular detail in the *C. elegans* model.

C. elegans shows developmental phenotypic plasticity: under conditions of ample food and optimal temperature, the worm develops to adulthood over four larval stages (L1–L4). However, when environmental conditions become unfavorable due to lack of food, overcrowding, or high temperature, the young larvae may decide to arrest in an alternative L3 stage, the dauer. This nonfeeding stage is characterized by a feeding and defecation arrest, altered metabolism (the use of internal fat stores), enhanced stress resistance, and long-term survival (128).

Despite its simple anatomy, *C. elegans* has a complex molecular biology that is supported by gene families that are often larger than those of other models (131) and humans. A few examples are the extended families of 39 insulin-like peptides (58, 93), 33 globins (55), and 81 cytochrome P450s (46). To some extent, this also applies to *C. elegans* redox-related enzymes such as superoxide dismutases (SODs). In contrast to the three SODs found in most other organisms, the *C. elegans* genome encodes five SODs, all of which are expressed (56). SOD-1, SOD-4, and SOD-5 are Cu/ZnSODs, while SOD-2 and SOD-3 are mitochondrial MnSODs. SOD-1 and SOD-2 are the major SODs in adult worms that are grown under nonstressing conditions. In dauers, transcription of SOD-1 and SOD-2 is suppressed while the other SODs are all highly upregulated (31, 56). SOD-4 is expressed as two alternatively spliced forms: SOD-4.1 is a secreted extracellular form and SOD-4.2 is an extracellular membrane bound form containing a transmembrane domain (43). The mitochondrial MnSODs SOD-2 and SOD-3 are associated with the I:III:IV supercomplex in the inner mitochondrial membrane (119).

All these specific spatial and temporal expression patterns and highly localized subcellular distribution of the different *C. elegans* SOD isoforms hint at complex ROS biology in this tiny animal. Taking into account these specific patterns, it seems unlikely that the five *C. elegans sod* genes have redundant functions. The lack of compensatory upregulation of alternative *sod* isoforms upon *sod* mutation supports this notion (7). However, in another study, upregulation of *sod-5* was observed upon *sod-1* mutation (133). Possibly, this *sod-5* upregulation was not a specific compensatory effect, but rather a general stress response to the knockout of the major SOD, elicited by insulin-like signaling (15, 31, 133).

Similar levels of complexity can be found in other redox-active enzymes, although they are less well-studied in *C. elegans*. The *C. elegans* genome contains a tandem array of three catalase (CTL) genes that show high sequence similarity. In addition, in this study, specific subcellular distribution of isoforms suggests highly specialized ROS and redox control. CTL-1 is expressed in the cytosol, while CTL-2 is a peroxisomal CTL that contributes 80% of the total CTL activity in the cell (92, 124). Less is known about the third CTL isoform.

The glutathione-*S*-transferase (*gst*) family in *C. elegans* is predicted to consist of 44 members for which function,

substrate, and localization are still to be determined in most cases. Several GSTs seem to be involved in oxidative stress resistance and detoxification of lipid peroxidation end products (5, 73).

In the *C. elegans* peroxiredoxin family, only *prdx-2* has been studied to some detail; it is abundantly expressed in distinct tissues (59) where it regulates stress-related functions *via* interaction with the insulin/insulin-like growth factor (IGF)-like signaling pathway and SKN-1 (Nrf2)-mediated stress response (26, 89, 90). It could potentially also function by direct reduction of redox-sensitive cysteines of proteins with diverse functions (71).

The *C. elegans* genome also encodes for several thioredoxins, thioredoxin reductases, and glutaredoxins, but its role in local redox signaling has received limited attention (36, 115); most of these genes were studied in relation to aging and their capacity to protect against oxidative stress (37, 61, 85).

ROS and redox reactions are of importance in growth and somatic maintenance of *C. elegans* as these reactions are involved in pathogen defense (21, 22, 53) and cuticle formation (33). However, detailed molecular information on specific ROS and redox signaling in *C. elegans* is scant. Several studies indicate that physiological levels of ROS influence *C. elegans* life span as a signaling molecule rather than a damaging agent (54, 134). For example, complex I inhibition was shown to extend life span by ROS generation and subsequent activation of the PMK-1/p38 mitogen-activated protein kinase pathway and SKN-1/Nrf2 in a specific set of neurons (106). In a similar way, life span extension in electron transport chain mutants is caused by increased mitochondrial ROS production and linked to the intrinsic apoptosis pathway. ROS-mediated activation of this pathway does not cause apoptosis, but activates a cell protective program (136). Furthermore, the subcellular site at which the ROS signal is generated in the mitochondrial mutants is of crucial importance to the life span phenotype (104).

Although the life span extension elicited by mitochondrial ROS is (partially) independent of the well-studied Insulin/IGF signaling pathway (106, 134), the downstream master regulator of Insulin/IGF signaling, DAF-16, is also redox regulated. Under oxidizing conditions, DAF-16 binds to the transportin-1 homolog IMB-2 by a disulfide bond and is translocated to the nucleus, independently of Ins/IGF signaling (96).

Besides aging- and stress-related processes, also development and sensory perception are under control of redox signaling. In *C. elegans clk-1*, a mutant that shows altered redox chemistry, germline development is delayed due to the oxidation of the low-density lipoprotein analog DSC-4, and a redox effect on both inositol 3-phosphate and *ras* signaling. In addition, vulval development is dependent on a cytoplasmic ROS signal that influences *ras* signaling (112). Redox-regulated sensory perception is illustrated by GLB-6, a neuronal globin that does not bind diatomic gas ligands, but rather transfers electrons. Because of these specific biochemical properties, it has been suggested to act in oxygen sensing *via* redox signaling (137). Another globin, GLB-12, was shown to generate a superoxide signal in the somatic gonad that is converted into a H_2O_2 gradient over the plasma membrane by intra- and extracellular SODs. This gradient was shown to influence several aspects of germline function, including apoptosis (27).

In summary, *C. elegans* is a very promising model for the study of ROS biology and redox signaling. Besides its general favorable characteristics as a model, it has an elaborate molecular machinery of redox-related enzymes that are probably involved in highly diverse biological processes. With the dawn of new technologies that allow detailed *in vivo* analyses of ROS and redox processes in this animal, an exciting period of discovery lies ahead.

First Explorations of *In Vivo* ROS and Redox Biology in *C. elegans*

Redox balance

The first redox-sensitive probes, termed reduction–oxidation-sensitive green fluorescent protein (roGFP) and rxYFP, were developed by the well-targeted insertion of disulfide bridges in GFP (30) and the yellow fluorescent protein (YFP) (91), respectively. This allowed the *in vivo* imaging and quantification of the dithiol–disulfide equilibrium in these proteins. The history and molecular properties of these early sensors, as well as their optimized successors, are reviewed in detail in refs. (84, 107). These probes have been used predominantly in cell cultures. A very first attempt to measure the redox status in live *C. elegans* using one of these probes was undertaken in 2010, in an experiment where roGFP1 was targeted to the mitochondria of the body wall muscles and intestine (63). In this study, it was shown that mitochondrial redox status can drastically change in mutants unable to undergo mitochondrial fusion at the level of the inner mitochondrial membrane, while this shift toward the oxidized state was not observed in mutants without fusion of the outer membrane. In a study on mitochondrial dynamics during and after anoxia, mitochondrially targeted roGFP was used to indicate mitochondrial oxidative stress in ventral cord neurites after a reoxygenation event (44).

Hydrogen peroxide

The earliest attempts to visualize and quantify H_2O_2 levels *in vivo* in real time in *C. elegans* were undertaken only a few years ago. In these studies, the genetically encoded sensor hydrogen peroxide sensor (HyPer) was expressed in transgene *C. elegans* reporter strains (6, 69). HyPer is a H_2O_2-specific biosensor and is created by combining the H_2O_2-sensitive regulatory domain of the *Escherichia coli* transcription factor OxyR with the circularly permuted YFP (cpYFP) (10). Exposure to H_2O_2 causes the formation of an intramolecular cysteine disulfide bridge within the OxyR regulatory domain, which results in a conformational change close to the cpYFP chromophore, changing its fluorescent properties. Oxidation of the sensor causes the 420-nm excitation peak to decrease and an increase of the 500-nm excitation peak, resulting in a 3- to 4-fold ratiometric shift. As the intramolecular disulfide bridge can be reduced by glutaredoxin activity, the probe can shift back to its original state and hence dynamic measurements of intracellular H_2O_2 levels can be made. The dynamic range and reaction kinetics of the HyPer probe were improved over the years (11, 81), but these newer versions—HyPer2 and HyPer3—have not been used in *C. elegans* yet.

Using HyPer, microscopic analysis of the spatial H_2O_2 patterns in the majority of the worm's tissues was possible by creating transgenic strains expressing the sensor under the constitutive promoter of the ribosomal large subunit *rpl-17*.

In young adult worms, the hypodermis, the body wall muscles, and the canal-associated neurons (CAN neurons) seem to be hot spots of H_2O_2 (6). Since the CAN neurons are associated with the excretory canals, H_2O_2 may be a signaling cue for osmoregulation. The increased H_2O_2 levels in the hypodermis are probably related to the presence of *Caenorhabditis elegans* dual oxidase, a H_2O_2-secreting transmembrane protein that is involved in tyrosine crosslinking of collagen in the cuticle (33). The high H_2O_2 levels that were observed in the body wall muscles may be an artifact as the experimental animals were paralyzed for confocal microscopy with levamisole, an acetylcholine receptor agonist of the body wall muscle cells causing tetanic contraction (4) and possible increase in H_2O_2 production (60). In older worms, these specific patterns disappeared and became more heterogeneous.

Ratiometric quantification of HyPer fluorescence by fluorimetry or image analysis showed an increase of H_2O_2 levels in aging worms in two independent studies (6, 69). At first sight, this seems to be in accordance with the oxidative stress theory of aging. However, it must be noted that the ROS increase at advanced age may be a consequence rather than a cause of aging. In worms that are long lived due to dietary restriction (6) or mutation in the insulin/IGF signaling receptor *daf-2* (69), the age-related H_2O_2 increase is attenuated. H_2O_2 levels seem to be much higher in juveniles than in adults (69), but this could not be confirmed in another study (6).

In a most recent study, the HyPer and roGFP sensors were targeted to different subcellular compartments and tissues to evaluate age-related deterioration of redox homeostasis. It was shown that the oxidized state inside the endoplasmic reticulum (ER) shifts toward a more reducing state during aging, while the redox state of the cytosol changes in the opposite way. These changes were aggravated by proteotoxic stress and proteasome inhibition. Tissue-specific experiments in neurons and muscle suggest that proteotoxic stress causes redox perturbation in a cell-nonautonomous manner (68).

The use of the HyPer probe for H_2O_2 quantification is not without controversy. As it is based on cpYFP, the fluorescence ratio is pH dependent in the range between 6 and 10, making it incompatible for comparison of samples or compartments that differ in pH (77). In such cases, alternative approaches should be followed, such as the simultaneous use of pH biosensors that operate at different wavelengths (122) or the calculation of the relative oxidation level of HyPer based on completely oxidized and reduced samples (78).

To overcome the pH dependency problem, another genetically encoded H_2O_2-sensor has been engineered: roGFP2-Orp1 (49, 84). roGFP2 is a redox-sensitive GFP with dual excitation and single emission properties with a stable fluorescence output within a physiological pH range of 5.8–8.0 (108). The Orp1 moiety of the protein, derived from yeast peroxidase, has cysteine residues that are specifically oxidized to a disulfide bridge by H_2O_2. The close proximity of roGFP2 to the Orp1 domain allows a very efficient dithiol–disulfide exchange, converting almost every H_2O_2 molecule into a roGFP2 disulfide bridge. Oxidation of the roGFP2 moiety can be quantified as it causes a shift in the fluorescence spectra. The sensor can be reduced by endogenous thioredoxins and probably also glutaredoxins, allowing dynamic measurements *in vivo* (2, 84). This promising H_2O_2 sensor has not been widely used in *C. elegans* research yet. One study, using a transgenic strain in which roGFP2-Orp1 was driven by the ubiquitous ribosomal protein promoter *rps-0*, reported that the H_2O_2 levels of long-lived worms cultured in axenic medium are comparable to those of control worms raised on *E. coli* bacteria (16). In a recent study, this sensor was used to quantify a H_2O_2 signal generated by the somatic gonad of the worm (27).

Superoxide

Although superoxide does not readily react with most biological molecules in aqueous solution, it quickly reacts with other radicals or enzymatic Fe–S clusters (51). It is biologically important as it is the precursor of the much more stable H_2O_2 and the potential source of the highly reactive hydroxyl radical. Due to its ephemeral properties, it is a molecule that is not easy to detect and quantify *in vivo*.

In 2008, cpYFP was proposed as a nonratiometric superoxide-specific sensor. When targeted to the mitochondria in cardiomyocyte cell cultures, specific boosts in fluorescence intensity (termed mitoflashes) could be observed (127). These cpYFP mitoflashes were also observed in the mitochondria of the *C. elegans* skin during wound healing. The generated ROS signal locally inhibits a Rho GTPase, which in turn allows actin remodeling and wound closure (132). In another *C. elegans* study, cpYFP mitoflashes were found as frequency peaks around the third and ninth day of adulthood (111). It was shown that life span of individual worms is inversely related to mitoflash frequency at the third day of adulthood, making mitoflash frequency a predictor of life span. However, whether cpYFP is a reliable indicator of superoxide is heavily debated as its fluorescent properties are also pH dependent (23, 57, 88, 109). As mitoflashes have also been observed with the pH sensor SypHer and the pH-independent superoxide probe MitoSOX^{TM} (97, 103), it cannot be excluded that both pH flashes and superoxide flashes occur in living mitochondria (64). Taking into account the importance of superoxide as a prime mitochondrial ROS and a precursor for H_2O_2 signaling, the development of new genetically encoded superoxide sensors with high sensitivity and specificity is highly needed.

Oxidized glutathione dimer:reduced glutathione redox balance

The tripeptide-reduced glutathione (GSH) is an omnipresent low molecular weight thiol that is often considered as a major ROS scavenger (32). All intermediates of the mammalian glutathione cycle were identified in *C. elegans* hinting at a common GSH metabolic network (3). As the intracellular GSH concentration is very high (1–11 m*M*) and the oxidized glutathione dimer (GSSG)/GSH ratio is usually below 1:100 in the cytoplasm (105), the redox state of the glutathione couple appears to be a good proxy for the total redox state in the cell. However, the use of the term ''total redox state'' is often discouraged as each redox couple in the cell is governed by its own kinetic control (107).

In vivo measurement of the intracellular GSH redox balance became within reach by the development of a roGFP2 sensor linked to the human glutaredoxin Grx1 (48). This coupling makes the response of roGFP2 to intracellular GSH redox status independent of endogenous glutaredoxins. Moreover, this tight link allows continuous equilibration between the $roGFP2_{red/ox}$ and GSSG/GSH redox pairs. The

mechanistic properties, specificity, reliability, and sensitivity of this sensor are discussed in detail in ref. (107).

The Grx1-roGFP2 sensor has been expressed in *C. elegans* to explore anatomical patterns and age-related changes in the redox status of the GSSG/GSH couple (6). In developing worms, a steady decline of the GSSG/GSH ratio was detected in the consecutive larval stages. The exact cause of this decrease is still unexplained, but may be linked to the gradual decrease of the number of differentiating cells (118), which are expected to have a high GSSG/GSH reduction potential (105).

Low GSSG/GSH ratios at the L4 and young adult stages may be a consequence of gametogenesis; GSH synthesis bursts were detected during mammalian gametogenesis (52). This idea is further supported by the fact that, in young adult worms, the spermatheca is the only structure that shows a significantly lower GSSG/GSH ratio compared to the rest of the worm (6). In mammals, GSH synthesis is not only increased in the gametes during gametogenesis and fertilization (100) but also in the surrounding tissues (9). This reducing environment in gametes and their surroundings appears to be evolutionary conserved. In addition, the *C. elegans* GSTs *gst-1* and *gst-4* are required for sperm maintenance in the spermatheca (70). In aging worms, the GSSG/GSH ratio tends to rise again (6). It is not clear whether this rise is causal to age-related deterioration or a secondary effect of aging. High intracellular glutathione levels are not sufficient to extend life span in *C. elegans* (121).

In a study where both roGFP1 and endogenous glutaredoxin activity were measured to estimate the GSH redox potential in *C. elegans*, it was found that the roGFP1 thiol–disulfide balance is sharply patterned within different tissues and varies strongly between isogenic individuals (101). These large fluctuations led to the idea that GSH is not the main cytosolic redox buffer, but rather acts as an amplifier of redox events affecting its oxidation state, *via* its redox potential. This, in turn, may affect the thiol–disulfide balance (and function) of many cytosolic target proteins. In the highly oxidizing ER, GSH may act as a redox buffer system.

Focus: ROS Signaling in the *C. elegans* Reproductive System

The C. elegans *gonad: general morphology and ROS signaling*

The *C. elegans* reproductive system consists of two bilaterally symmetric U-shaped gonad arms that are connected to a central uterus through the spermathecae. The distal part of the germline is a syncytium containing approximately thousand nuclei in cup-shaped hexagonal compartments open to a cytoplasmic core, the rachis. During progression toward the proximal region of the germline, compartments mature, nuclei become meiotic, and, as they pass through the bend of the gonad arm, enlarge, cellularize, and further mature to oocytes. These oocytes are fertilized by sperm (formed during L4 stage) when passing through the spermatheca. Following fertilization, the zygotes become surrounded by a vitelline membrane and eggshell and start embryogenesis in the uterus, after which they are expelled through the midventral vulva.

In the gonad arms, the germline is surrounded by a thin layer of somatic sheath cells. The intimate association between sheath cells and germline is of primary importance for the orchestration of development, organization, and function of the germ cells (50, 82). Paracrine signaling between the somatic gonad and germline has been well studied (67, 75). In addition, several observations indicate that redox signaling is intimately associated with the regulation of *C. elegans* reproduction: maturing oocytes display an increase in ROS levels that is associated with mitochondrial activity, SOD-1 activity, and fertilization (135), altered redox chemistry of a mitochondrial mutant influences several signaling cascades associated with germline development (112), and the spermatheca shows a more reduced glutathione redox status compared to other tissues (6).

Very recently, several proteins involved in a gonadal redox signaling cascade have been identified by our group. In the gonadal sheath cells, a superoxide-generating globin (GLB-12) is anchored in the plasma membrane by myristoylation and palmitoylation. The local superoxide signal generated by this globin is converted to what appears to be a H_2O_2 gradient over the plasma membrane by the activity of intracellular and extracellular SODs. In turn, this H_2O_2 gradient influences overall fecundity, gonad morphology, and the rate of physiological germline apoptosis *via* the JNK/p38 pathways (27). While the superoxide-generating capacity of the globin was demonstrated by an *in vitro* biochemical approach, the H_2O_2 signal was measured *in vivo* by means of the roGFP2-Orp1 biosensor. Expression of this biosensor was driven by the *glb-12* promoter to ensure close proximity of the sensor to the native GLB-12 protein. H_2O_2 was quantified by ratiometric analysis of fluomicrographs taken at 405- and 488-nm excitation wavelengths. This approach allowed quantification of very local H_2O_2 signals in a very thin layer of gonadal sheath cells.

Exploring in vivo *H_2O_2 patterns in the* C. elegans *germline*

As the *C. elegans* gonad appears to be a complex yet accessible organ in which probably multiple types of redox signaling occur, we decided to analyze the pattern of H_2O_2 levels in the germline under both normal conditions and following exogenous oxidative stress.

The expression of transgenes in the *C. elegans* reproductive system is particularly difficult due to germline silencing of genes lacking the necessary regulatory sequences. Therefore, the *roGFP2-Orp1* gene was optimized to allow its expression in this tissue. This approach was based on the thoroughly described optimization of enhanced green fluorescent protein (*eGFP*) and *mCherry* for *C. elegans* (germline) expression (47). In short, this consisted of (i) introducing artificial intronic sequences, identical to those used in *eGFP* and *mCherry*, and (ii) adapting codon usage to 60% of most optimal usage in *C. elegans* to achieve higher expression. This was carried out by using the software ''*C. elegans* Codon Adapter'' (http://worm-srv3.mpi-cbg.de/codons/cgi-bin/optimize.py). The latter approach has also been described as a way to control protein levels, whereby the relative amount of optimal codons determines the expression level of the protein (99). Finally, an *fbf-1* promoter and *tbb-2* 3′UTR combination that leads to expression in the entire germline (83) was chosen to drive expression of the *roGFP2-Orp1* gene (Fig. 1A, B). Engineered transgenes were cloned into pCFJ150 and injected into strain EG6699 to create

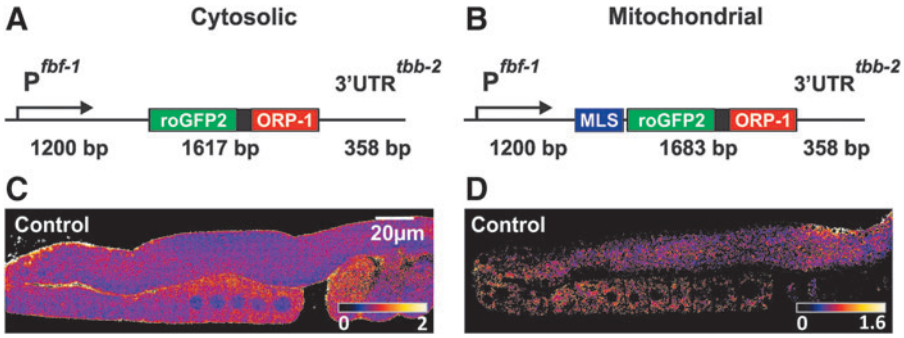

FIG. 1. Expression of roGFP2-Orp1 in the *Caenorhabditis elegans* germline. Schematic overview of the cytosolic **(A)** and the mitochondrial **(B)** roGFP2-Orp1 gene construct. Ratiometric image of cytosol **(C)** and mitochondrial **(D)** roGFP-Orp1 in the gonad of intact living animals. Both images show the gradual increase in H_2O_2 levels from the distal (*upper*) part toward the proximal (*lower*) part of the gonad. H_2O_2, hydrogen peroxide; MLS, mitochondrial localization sequence; roGFP, reduction–oxidation-sensitive green fluorescent protein

integrated single-copy *roGFP2-Orp1* transgenes using the mos1-mediated single copy insertion (MosSCI) method (41).

In this set of experiments, *C. elegans* was cultured at 20°C on cholesterol-supplemented nutrient agar (OXOID) plates containing a lawn of freshly grown *E. coli* OP50 cells (116).

To study H_2O_2 levels in the *C. elegans* germline, roGFP2-Orp1 was targeted to either the cytosol or the mitochondrial matrix within the germline (Fig. 1C, D). While roGFP2-Orp1 has an approximately eight-fold dynamic range under ideal conditions (49), the experimental dynamic range can be influenced by a number of parameters, such as microscope sensitivity, interfering background fluorescence, and probe expression levels. The experimental dynamic range was determined by exposing living worms to an excess of dithiothreitol and H_2O_2 to achieve complete reduction and oxidation of the probe, directly followed by measuring the emission intensity and optimizing microscope settings (87) (Fig. 2).

One-day-old adult hermaphrodites were used, which were anesthetized for 15–30 min in a fresh mixture of 1 mg/ml Tricaine and 0.1 mg/ml tetramisole hydrochloride dissolved in M9 before transferring them to an agarose pad under a coverslip for imaging. Gonads were imaged by collecting a 10×2 mm z-series following excitation at 405 and 488 nm. Microscopy was performed with a Nikon Eclipse TE2000-5 confocal microscope. All image processing was carried out as described by Morgan *et al.* (87). In brief, images were saved as 16-bit tiff files and processed by ImageJ. Images were first converted to 32-bit tiff files, background was subtracted using an upper and lower threshold, and background values were set to ''not a number.'' Subsequently, 405-nm images were divided by 488-nm images pixel by pixel to create the ratio images, and displayed in false colors using the lookup table ''Fire''. Relative H_2O_2 levels in these processed images were quantified by selecting eight equally sized rectangle areas in a single focal plane, followed by the calculation of the mean ratio in each of the selected areas (Fig. 5A).

Following determination of the dynamic range, the cytosolic and mitochondrial probes were used to visualize H_2O_2 levels within the germline under normal nonstressing conditions, also in living, anesthetized, 1-day-old adult hermaphrodites. Both probes showed a remarkable spatial H_2O_2 pattern within the germline: H_2O_2 levels tend to increase toward the proximal side of the germline and peak within oocytes before fertilization and in the zygote directly following fertilization (Figs. 1C, D, and 3A, B). From the two-cell embryo onward, H_2O_2 levels decrease again. The H_2O_2 increase in the proximal germline corresponds with the previously described ROS increase detected in maturing oocytes (135). Noteworthy, in that study, the ROS increase was dependent on SOD-1 activity, suggesting that a considerable amount of this ROS consists of $O_2^{\bullet -}$ or H_2O_2.

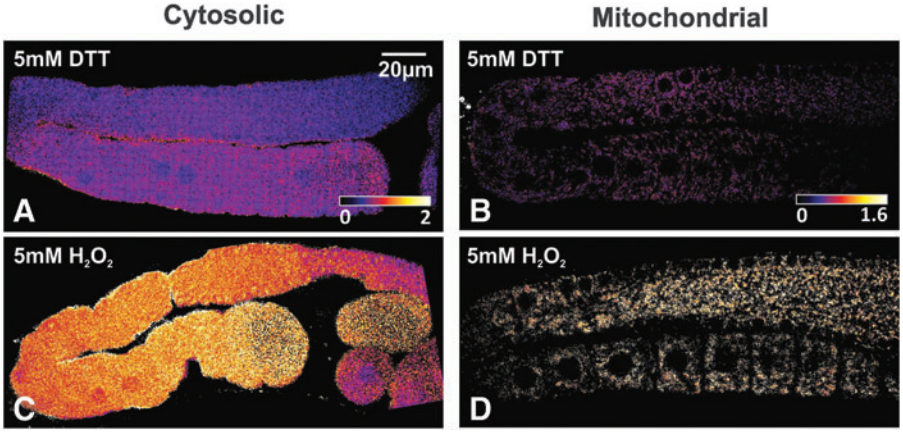

FIG. 2. Determining the experimental dynamic range of roGFP2-Orp1 in the *C. elegans* germline. Ratiometric image of the gonad arm in intact living animals under reducing **(A, B)** and oxidizing **(C, D)** conditions of worms expressing roGFP-Orp1 in the cytosol **(A, C)** and in the mitochondria **(B, D)**. Reducing conditions were obtained by exposing the worms to 5 m*M* DTT immediately before imaging; oxidizing conditions were obtained with 5 m*M* H_2O_2 immediately before imaging. DTT, dithiothreitol.

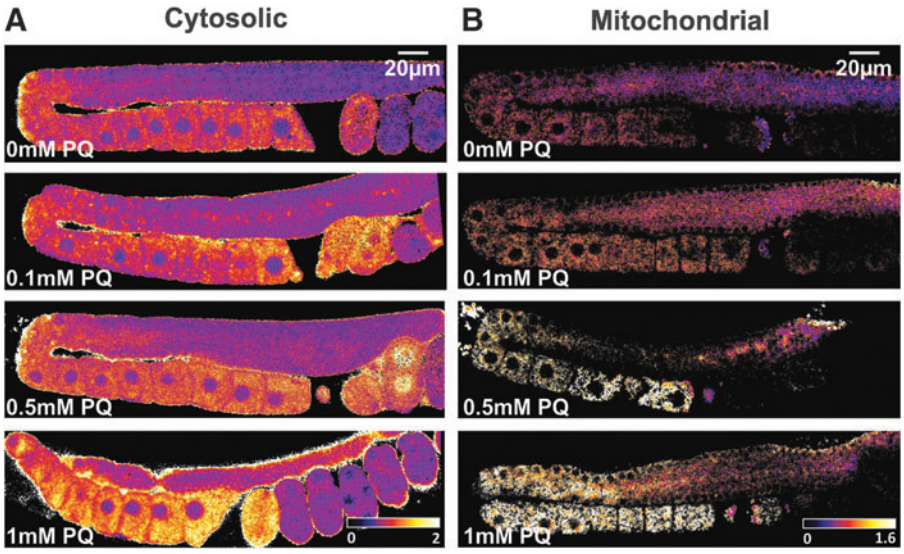

FIG. 3. To increase mitochondrial H_2O_2 production, worms were exposed to several concentrations of PQ for 24 h before imaging. Following this treatment, ratiometric images of the cytosolic **(A)** and the mitochondrial **(B)** roGFP2-Orp1 probe in the gonad of living animals showed that H_2O_2 levels were increased in both the cytosol and inside mitochondria compared to the control condition. PQ, paraquat.

The cytosol-targeted probe is also present in the oocyte nuclei and indicates that nuclear H_2O_2 levels are lower compared to cytosolic levels (Figs. 1C, 3A, and 4A). Cellular compartmentalization of H_2O_2 has been observed before (77, 86), and it is assumed that the permeability of plasma membranes to H_2O_2 is actively regulated (18, 28, 38). However, nuclear pores are transparent to small molecules such as H_2O_2. The clear lack of H_2O_2 in the oocyte nucleus may reflect the absence of SOD in this organelle. Although slightly smaller than the 40-kDa cutoff limit in vertebrates (79), cytosolic SOD dimers ($\sim$32 kDa) (62) may be too large to diffuse passively through the nuclear pore in *C. elegans*. Overall, these results show that spatial differences in H_2O_2 levels are present within the *C. elegans* germline under normal conditions and suggest that H_2O_2-based redox signaling may indeed be present in this tissue.

Visualization of manipulated ROS levels in the C. elegans *gonad*

Next, we analyzed if (i) paraquat and (ii) RNAi against a mitochondrial protein would lead to detectable changes in H_2O_2 levels.

Paraquat can act as a redox cycling compound and causes increased $O_2^{\bullet-}$ production within the mitochondria (12, 17). This leads to oxidative stress and premature death when paraquat is present at high levels, but results in life span extension when used at low levels, potentially by modifying redox-sensitive signaling pathways (72, 125). Paraquat is therefore a useful compound to analyze both the beneficial and detrimental effects of ROS.

The second approach, depletion of mitochondrial proteins, generally causes mitochondrial stress and is often associated with increased mitochondrial ROS production. Similar to paraquat, partial depletion of mitochondrial proteins can have beneficial effects, while stronger depletion is almost always harmful (98). However, the level of depletion to induce beneficial effects is a priori not known and varies between different mitochondrial proteins.

For this analysis, we chose to use both beneficial (0.1–0.25 m*M*) and harmful (>0.25 m*M*) concentrations of paraquat (72, 125) and to deplete the mitochondrial protein ASB-1, a germline-specific ATP-synthase subunit. Because ASB-1 is only present in the germline, ASB-1 depletion does not affect somatic mitochondria and worms develop at a normal rate and do not show any defects other than those of the

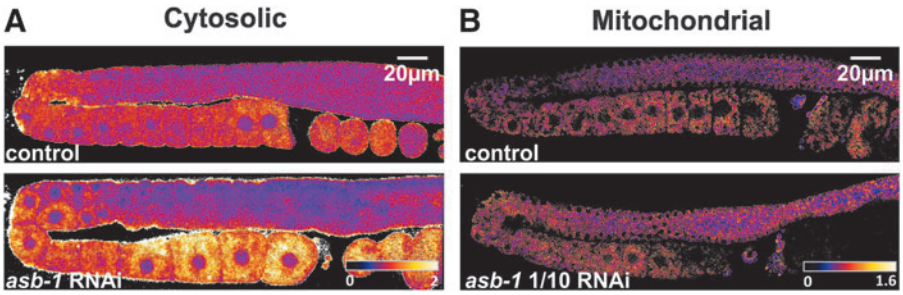

FIG. 4. To analyze the effect of mitochondrial stress on H_2O_2 levels, worms were exposed to RNAi against the mitochondrial germline-specific protein ASB-1 for 24 h before imaging. Depletion of ASB-1 caused a clear increase in cytosolic H_2O_2 levels **(A)**. Undiluted *asb-1* RNAi arrested import of the mitochondrially targeted roGFP2-Orp1 (not shown), while with 1/10 diluted *asb-1* RNAi, roGFP2-Orp1 was still targeted to the mitochondria, but no changes in H_2O_2 levels could be observed **(B)**. RNAi, RNA interference.

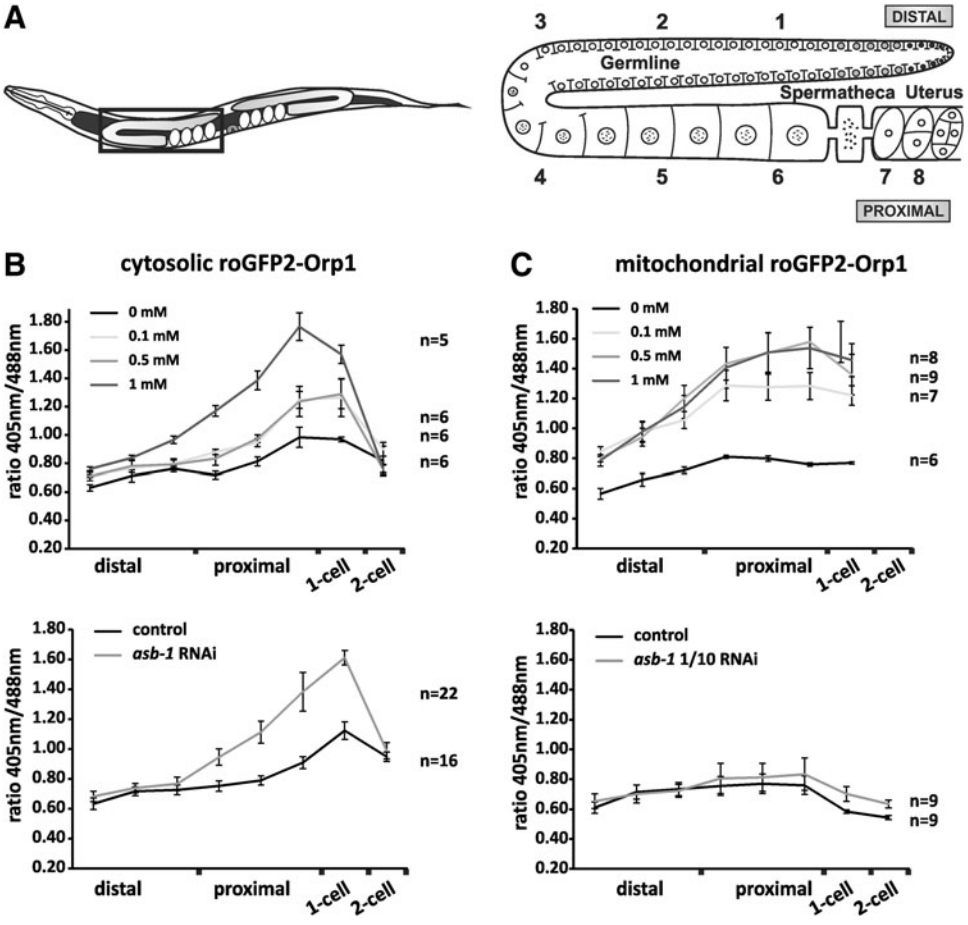

FIG. 5. The *C. elegans* germline shows a H_2O_2 gradient. **(A)** Schematic overview of the *Caenorhabditis elegans* germline, showing the regions where relative H_2O_2 levels were quantified. Regions 1–3 correspond to measurements in the distal germline, 4–6 to the proximal germline, 7 to one-cell embryos, and 8 to two-cell embryos. To calculate and plot relative H_2O_2 levels in the cytosol **(B)** and mitochondria **(C)**, ratiometric images of individual gonads were generated, after which the roGFP-Orp1 ratiometric signal was measured in these eight different regions. In control conditions, both the cytosolic and mitochondrial H_2O_2 levels show a gradual increase from the distal toward the proximal region of the gonad, followed by a decrease in the two-cell embryo. These spatial differences in H_2O_2 levels became more pronounced when animals were exposed to paraquat (*upper panels*), and, specifically for cytosolic H_2O_2 levels, also when worms were treated with *asb-1* RNAi (*lower panels*).

germline (65). However, it is not known if partial depletion of this protein can have beneficial effects in the organism.

A freshly made paraquat stock solution was added into Nematode growth medium (NGM) the day before the plates were used, while feeding RNAi was used to knockdown *asb-1* (123). For both treatments, synchronized L4 worms were exposed for 24 h to either condition before imaging. Also in these experiments, living anesthetized hermaphrodites were used for imaging.

Both paraquat exposure and *asb-1*(*RNAi*) resulted in increased cytosolic H_2O_2 levels, which were most pronounced in the proximal germline and the one-cell embryo (Figs. 3A, 4A, and 5A, B). Paraquat treatment also caused increased H_2O_2 levels in the mitochondrial matrix, with a spatial distribution that is comparable to this of cytosolic H_2O_2 levels (Figs. 3B, 4B, and 5A, C). No changes in H_2O_2 levels in the mitochondrial matrix were observed following ten times diluted *asb-1* RNAi (Figs. 4B and 5C). Unfortunately, less diluted *asb-1* RNAi affected mitochondrial function to such an extent that mitochondrial protein import of roGFP2-Orp1 was severely reduced (not shown). While the disturbed mitochondrial import clearly shows that *asb-1* RNAi interferes with normal mitochondrial function, at the same time it precludes accurate assessment of H_2O_2 levels in the mitochondrial matrix.

Remarkably, H_2O_2 levels in the oocyte nuclei seemed nearly unaffected by the paraquat and *asb-1*(RNAi) treatment (Figs. 3A and 4A). This further supports the above-mentioned assumption that the oocyte nucleoplasm lacks SOD activity. In agreement with this, H_2O_2-treated worms do show similar H_2O_2 levels inside and outside the oocyte nuclei (Fig. 2C). Another striking spatial pattern is the sudden drop in H_2O_2 levels after the first or second embryonic cell division. Even when H_2O_2 levels in the cytosol were raised by paraquat treatment or *asb-1*(*RNAi*), they dropped to near-baseline levels at the two-cell stage (Fig. 5B). This drop may be the result of the sudden increase in CTL expression in very young embryos (74). Low expression or absence of CTL in the earlier stages may allow efficient H_2O_2 signaling during gametogenesis (27, 135).

Overall, quantification of gonadal H_2O_2 by image analysis using the roGFP2-Orp1 probe was very reproducible (Fig. 5). The ability to detect the increase in H_2O_2 levels in worms treated with 0.1 m*M* paraquat, a concentration known to inflict a hormetic effect (72, 125), suggests that the roGFP2-Orp1 probe in the *C. elegans* germline can be used to study redox signaling events. Sensitivity of this sensor to redox signaling has also been confirmed in other systems such as *Drosophila* and HeLa cells (2, 49). In addition, because the additional H_2O_2 increase at higher, harmful paraquat concentrations is also within the dynamic range of the roGFP2-Orp1 probe, this system could potentially be used to analyze both the effects of H_2O_2 in redox signaling and in oxidative stress.

In conclusion, these explorative results support the potential of the *C. elegans* reproductive system as a model to study redox signaling in a complex tissue. Spatial patterns in

H_2O_2 levels are clearly visible under normal conditions while changes in H_2O_2 levels due to RNAi-induced mitochondrial perturbation and mild or severe paraquat treatment are easily quantifiable in a reproducible way.

Limitations and Pitfalls

The development of genetically encoded redox sensors has greatly advanced our understanding of redox biology at the cellular and organismal level. As their potential has been only used by few in *C. elegans* redox biology, these tools will undoubtedly lead to more important discoveries in worm redox biology in the near future. However, these promising tools also have their limitations, and sensor data should always be interpreted with care.

The Sensors

General limitations and shortcomings of the genetically encoded redox sensors were recently reviewed in detail in ref. (107). Redox sensors have their specific measuring range beyond which they cannot detect any redox shifts. In addition, the sensor's (non-)specificity should be taken into account as some are linked to protein domains with high substrate specificity (*e.g.*, Grx1 for GSSG/GSH and Orp1 for H_2O_2), while other sensors rely on endogenous glutaredoxin activity for equilibration with the GSSG/GSH redox couple. Interactions with other redox systems cannot be ruled out, and even nonrelated properties, such as pH, may influence the probe. This is especially relevant for the YFP-based sensors. In addition, the quantum yield of the roGFP2- and HyPer-based probes is lower at certain wavelengths compared to the standard EGFP, demanding higher sensitivity of the applied detection systems.

Transgenic Worm Strains

C. elegans has a very long history in transgenesis (117) and it was the first animal in which GFP was heterologously expressed (19). The most easy and common method for *C. elegans* transgenesis is microinjection of a transcriptional or translational construct, together with a selection marker in the gonad. This approach most often yields transgenic progeny with a multicopy extrachromosomal array with variable transmission (35). In some cases, spontaneously integrated lines can be selected or integration can be induced by ultraviolet (UV) treatment (80).

These multicopy transgenic strains may show strong expression of the sensor, which is advantageous for obtaining clear fluorescence readouts. However, strong heterologous expression may cause deleterious phenotypes in the transgenic worms. The molecular underpinnings of these effects are often unknown, but may relate to the heavy burden on transcriptional and translational machinery or, in case of fusion sensors, the influence of the active redox moieties of the sensor on the intracellular environment. Hence, it is recommended that the transgenic sensor strains are tested for sensitive life history traits such as life span, fecundity, and motility.

Low- or single-copy integration of the sensor construct in the *C. elegans* genome may overcome some of the problems mentioned previously. Low-copy integration has been achieved by biolistic bombardment strategies (94), but similar to UV-induced integration, construct integration happens randomly and may occur in the coding region or regulatory elements of a gene, thereby creating an insertion mutant. More recent genome editing tools such as MosSCI (41) and clustered regularly interspaced short palindromic repeats/CRISPR-associated CrRNA 9 (CRISPR/Cas9) (40) allow a site-specific single-copy insertion of the sensor gene in the *C. elegans* genome and are therefore to be preferred.

The transgenic lines presented in the previous section were created by MosSCI genome editing (see Supplementary Materials; Supplementary Data are available online at www.liebertpub.com/ars), proving for the first time that this method allows the development of stable transgenic strains expressing biosensors at levels that can be easily visualized and quantified. To maximize expression of this single copy, the sensor gene was codon-optimized as described previously (see also Supplementary Materials). For now, the CRISPR/Cas9 method has not yet been applied for the generation of new *C.elegans* redox sensor strains, but undoubtedly such strains will be developed soon.

As ROS signals or redox balances may act very locally (27, 86), it is important to target the sensor as closely as possible to the area of interest to obtain a clear readout. This can be done by targeting the sensor to specific tissues or cellular compartments (68). In a recent study, the roGFP2-Orp1 sensor was expressed in very close proximity to the low–abundant superoxide generator globin-12 in *C. elegans* (27). This was achieved by fusing the sensor gene to the upstream and downstream region of the *glb-12* gene, together with the sequence coding for the first 30 amino acids of GLB-12. This N-terminal sequence contains a myristoylation and palmitoylation site, probably anchoring the sensor in lipid rafts in the plasma membrane of the target cells, in very close proximity to the GLB-12 superoxide generator, offering maximal sensitivity to the weak ROS signal.

Analysis of the Ratiometric Fluorescence Signal

The fluorescence signal of the redox sensor can be quantified by direct fluorimetry (*e.g.*, in a microplate reader) or by image analysis of fluorescence micrographs. In the experimental protocol of both approaches, the preparation steps may impose stress upon the worms and may influence internal redox balances. Therefore, all samples should be handled identically; preparation steps should be carefully timed and carried out in a way that minimizes the stress burden (avoiding dehydration during worm picking, temperature stress on a microscope stage, hypoxia in densely populated microwells, food deprivation, and so on).

Autofluorescence can be a confounder in ratiometric fluorimetry of redox sensors. Unfortunately, in *C. elegans*, the hypodermal nucleoli and especially the gut granules have autofluorescent properties (13), the latter being caused by accumulation of anthranilic acid glucosyl esters (24). Hence, micrographs showing any ratiometric signal in these structures should be interpreted with care. In such images, autofluorescence can be estimated by excitation of the sample in a wavelength range outside the excitation range of the probe (39). In case of cell- or tissue-specific analysis, regions of interest outside the autofluorescent areas can be selected (69). In quantitative fluorimetry, autofluorescence may be (partially) controlled for by using matched worm strains that do

not contain the sensor (6). As *C. elegans* does not show any red autofluorescence, redox sensors emitting in the long wavelength range would be the optimal solution. Only one such sensor, the H_2O_2-sensitive HyPerRed, is currently available, but, unfortunately, it is based on the pH-sensitive circularly permuted mApple fluorophore (34).

Microplate-based fluorimetry allows high-throughput quantification of large worm populations in many parallel samples. In this type of setup, worm density in the microplate wells should be considered with care: low densities may not yield enough signal, while high densities may cause hypoxia to the worms. The ratiometric properties of the sensors make them less sensitive to differences in expression levels, photobleaching, and worm density in the well. However, widely differing worm densities within and between experiments should be avoided.

To explore these density effects, we set up a worm dilution experiment in a microplate using three sensors. *In vivo* H_2O_2 levels were quantified using *jrIs1[rpl-17p::HyPer], jrIs10 [unc-119(+) rps-0p::roGFP2-Orp1]*, and the glutathione redox potential was determined with the strain *jrIs2[rpl-17p::Grx1-roGFP2]* (6, 16). All strains were age synchronized *via* bleaching and scaled up on nutrient agar plates seeded with *E. coli* K12 bacteria at 20°C. Day 1 adults were washed twice with S-basal, and the dense worm suspension was distributed as a linear dilution series (5–100%) over at least 10 wells of a black microtiterplate. H_2O_2 levels and the glutathione redox potential in live worms were determined *via* a fluorimetric assay as described in ref. (6). Fluorescence was measured over a 30-min period at 25°C using a Wallac Victor^2 Multilabel Counter (PerkinElmer, Boston, MA) with 405- and 490-nm excitation filters and a 535-nm emission filter. For each sample, data were averaged over the 30-min measurement period. Data of at least three biological replicates were pooled per strain.

This dilution experiment showed that fluorescence intensities at both excitation wavelengths do not increase proportionally (Fig. 6A). The weak exponential relation between both fluorescence intensities results in increased fluorescence ratios at low worm densities (*i.e.*, at low sensor levels and low fluorescence intensity). This deflection is apparent only at very low worm densities and becomes negligible as densities increase (Fig. 6B). Hence, we generally recommend that only samples with similar worm densities should be compared. Finally, autofluorescence or absorption properties of experimental compounds added to the wells may affect the ratiometric signal and make comparison with untreated controls illegitimate.

Ratiometric imaging requires the capture of two separate perfectly overlapping images. As *C. elegans* is a very motile species, adequate measures should be taken to prevent worm movement during image capturing (126). Anesthetics such as sodium azide, levamisole/tetramisole, and tricaine (MS-222) are frequently used in worm microscopy. Sodium azide is a potent mitochondrial inhibitor known to induce *gst-4*, a marker of oxidative stress (76), and thus should be avoided as an anesthetic in redox assays. Levamisole is a nicotinic acetylcholine receptor agonist causing tetanic paralysis. It is not known whether permanent muscle contraction in *C. elegans* causes oxidative stress, but the effects are probably less severe compared to sodium azide. Tricaine is a neurotoxin that acts as a

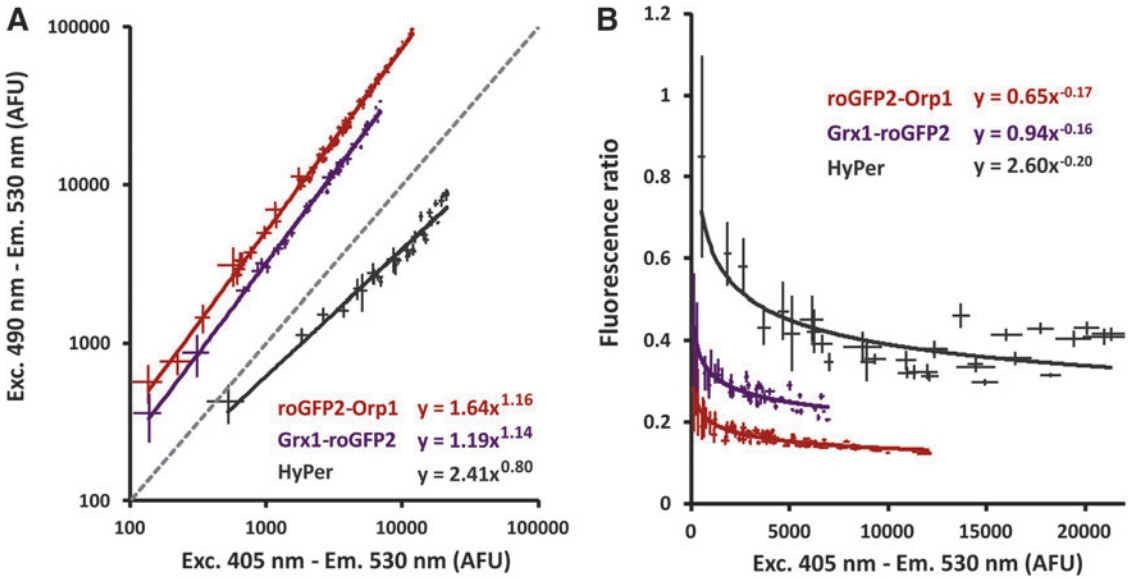

FIG. 6. Density effects in microplate-based fluorimetry of large worm populations. **(A)** Nonlinear correlation of green fluorescence (530 nm) after violet (405 nm) and blue (490 nm) excitation of the sensors roGFP2-Orp1, Grx1-roGFP2, and HyPer. At least three independent replicate populations of each worm strain were diluted. Each symbol represents a single dilution of a given replicate experiment. The symbols consist of vertical and horizontal standard deviations calculated as the fluctuation of 13 consecutive fluorescence measurements over a 20-min time period. **(B)** Fluorescence ratio plotted against sensor concentration (estimated by fluorescence intensity following violet excitation in varying population densities of unstressed worms expressing the roGFP2-Orp1, Grx1-roGFP2, or HyPer sensor). At low sensor concentrations, the fluorescence ratio tends to show an incline. Fluorescence ratios were calculated as the 405/490 nm signal for roGFP2-Orp1 and Grx1-roGFP2, and as the 490/405 nm signal for HyPer. HyPer, hydrogen peroxide sensor.

muscle relaxant. Agar pads (66, 110) are often used to glue worms to a microscope slide and have the advantage of being a nontoxic to the worms.

One of the most promising techniques in this area is the use of microfluidics, which allows fixation of individual worms without anesthetics and, depending on the chip design, real-time feeding or compound treatment (102). A well-designed microfluidics chip would also allow imaging of treated and control worms in one microscopic field, thereby eliminating small variations that may occur in different preparations and that affect ratiometric imaging.

In ratiometric redox imaging, two images, taken at different excitation wavelengths, are compared. As perfect overlay is necessary, the lens system of the microscope should be sufficiently corrected for chromatic aberration within the respective wavelength ranges. If not, this may result in ratiometric ''fringing'' effects that should be interpreted with care. Among other hardware-related issues, the dynamic range of the photodetection device is noteworthy. This range should be wide enough to discriminate small differences in fluorescence intensity from the low- to high-intensity range. During image capturing, pixel saturation should be avoided as this leads to ratio capping (126).

Finally, several software packages can be applied for processing the raw fluomicrographs, ranging from dedicated program packages included in the microscope software, open source packages such as Fiji (W. Rasband; NIH, Bethesda, MD), to advanced software pipelines reviewed in ref. (39). Ratiometric images can be presented in different standard pseudocolor schemes. However, one of the most intuitive representations is the intensity-normalized ratio (INR) image (6). This is a hue saturation value image in which the hue represents the ratio of both fluorescence channels while the value is calculated as the average intensity of both fluorescence channels. Hence, regions with low fluorescence intensity (and thus high noise levels and less useful information) will appear dim in the INR image, attracting less attention. Regions with high fluorescence intensity, allowing more solid ratiometric measurements, appear in more intense colors. Currently, real-time INR imaging is only implemented in the Nikon NIS elements software, but INR images can also be calculated *post hoc via* Fiji software.

Future Perspectives

Over the last decade, the field of redox biology has greatly benefitted from the development of genetically encoded redox sensors as they have many advantages over classical ROS probes. Obviously, in this young research field, there are ample opportunities for improvement and many suggestions have been forwarded in outstanding reviews (14, 84, 107). Within the *C. elegans* research community, the following issues are probably on top of the wish list:

- Extension of the family of redox sensors with members (i) that have emission spectra in the red range avoiding interference with autofluorescence, (ii) are highly specific and sensitive to the most commonly studied ROS and redox couples [superoxide, H_2O_2, GSSG/GSH, NAD(P)/NAD(P)H, ..], and are not influenced by pH.
- Practical solutions for dynamic ratiometric analysis in *C. elegans*. This issue may be solved by combining microscopes built for fast four-dimensional (4D) fluorescence imaging (95) and genetically encoded sensors that allow emission ratiometry rather than excitation ratiometry (14). Using dichroic emission filter set, this would allow capturing the two fluorescence images simultaneously and increase time resolution of the 4D recording. Ideally, this should be combined with efficient nontoxic fixation of juxtaposed control and treated worms in a microfluidic device.

Acknowledgments

The authors are grateful to Karen Oegema and members of the OD laboratory for their advice and support in generating the germline roGFP2-Orp1 probes. Grx1-roGFP2 in the bacterial expression vector pQE-60 was kindly provided by T.P. Dick. Some strains were provided by the CGC, which is funded by the NIH Office of Research Infrastructure Programs (P40 OD010440). S.D.H. was a PhD fellow of the Fund for Scientific Research (FWO). P.B. was PhD fellow indebted to the Institute for the Promotion of Innovation through Science and Technology in Flanders (IWT-Vlaanderen).

References

1. *C. elegans* Sequencing Consortium. Genome sequence of the nematode *C. elegans*: a platform for investigating biology. *Science* 282: 2012–2018, 1998.
2. Albrecht SC, Barata AG, Grosshans J, Teleman AA, and Dick TP. In vivo mapping of hydrogen peroxide and oxidized glutathione reveals chemical and regional specificity of redox homeostasis. *Cell Metab* 14: 819–829, 2011.
3. Asamoto H, Ichibangase T, Saimaru H, Uchikura K, and Imai K. Existence of low-molecular-weight thiols in *Caenorhabditis elegans* demonstrated by HPLC-fluorescene detection utilizing 7-chloro-N-[2-(dimethylamino)ethyl]-2,1,3-benzoxadiazole-4-sulfonamide. *Biomed Chromatogr* 21: 999–1004, 2007.
4. Avery L and Horvitz HR. Effects of starvation and neuroactive drugs on feeding in *Caenorhabditis elegans*. *J Exp Zool* 253: 263–270, 1990.
5. Ayyadevara S, Engle MR, Singh SP, Dandapat A, Lichti CF, Benes H, Shmookler Reis RJ, Liebau E, and Zimniak P. Lifespan and stress resistance of *Caenorhabditis elegans* are increased by expression of glutathione transferases capable of metabolizing the lipid peroxidation product 4-hydroxynonenal. *Aging Cell* 4: 257–271, 2005.
6. Back P, De Vos WH, Depuydt GG, Matthijssens F, Vanfleteren JR, and Braeckman BP. Exploring real-time in vivo redox biology of developing and aging *Caenorhabditis elegans*. *Free Radic Biol Med* 52: 850–859, 2012.
7. Back P, Matthijssens F, Vlaeminck C, Braeckman BP, and Vanfleteren JR. Effects of sod gene overexpression and deletion mutation on the expression profiles of reporter genes of major detoxification pathways in *Caenorhabditis elegans*. *Exp Gerontol* 45: 603–610, 2010.
8. Bartosz G. Use of spectroscopic probes for detection of reactive oxygen species. *Clin Chim Acta* 368: 53–76, 2006.
9. Beck MJ, McLellan C, Lightle RL, Philbert MA, and Harris C. Spatial glutathione and cysteine distribution and

chemical modulation in the early organogenesis-stage rat conceptus in utero. *Toxicol Sci* 62: 92–102, 2001.
10. Belousov VV, Fradkov AF, Lukyanov KA, Staroverov DB, Shakhbazov KS, Terskikh AV, and Lukyanov S. Genetically encoded fluorescent indicator for intracellular hydrogen peroxide. *Nat Methods* 3: 281–286, 2006.
11. Bilan DS, Pase L, Joosen L, Gorokhovatsky AY, Ermakova YG, Gadella TW, Grabher C, Schultz C, Lukyanov S, and Belousov VV. HyPer-3: a genetically encoded H(2)O(2) probe with improved performance for ratiometric and fluorescence lifetime imaging. *ACS Chem Biol* 8: 535–542, 2013.
12. Blanco-Ayala T, Anderica-Romero AC, and Pedraza-Chaverri J. New insights into antioxidant strategies against paraquat toxicity. *Free Radic Res* 48: 623–640, 2014.
13. Boulin T, Etchberger JF, and Hobert O. Reporter gene fusions. *WormBook* 5: 1–23, 2006.
14. Breckwoldt MO, Wittmann C, Misgeld T, Kerschensteiner M, and Grabher C. Redox imaging using genetically encoded redox indicators in zebrafish and mice. *Biol Chem* 396: 511–522, 2015.
15. Cabreiro F, Ackerman D, Doonan R, Araiz C, Back P, Papp D, Braeckman BP, and Gems D. Increased life span from overexpression of superoxide dismutase in *Caenorhabditis elegans* is not caused by decreased oxidative damage. *Free Radic Biol Med* 51: 1575–1582, 2011.
16. Castelein N, Muschol M, Dhondt I, Cai H, De Vos WH, Dencher NA, and Braeckman BP. Mitochondrial efficiency is increased in axenically cultured *Caenorhabditis elegans*. *Exp Gerontol* 56: 26–36, 2014.
17. Castello PR, Drechsel DA, and Patel M. Mitochondria are a major source of paraquat-induced reactive oxygen species production in the brain. *J Biol Chem* 282: 14186–14193, 2007.
18. Chaiswing L and Oberley TD. Extracellular/microenvironmental redox state. *Antioxid Redox Signal* 13: 449–465, 2010.
19. Chalfie M, Tu Y, Euskirchen G, Ward WW, and Prasher DC. Green fluorescent protein as a marker for gene expression. *Science* 263: 802–805, 1994.
20. Chattoraj M, King BA, Bublitz GU, and Boxer SG. Ultrafast excited state dynamics in green fluorescent protein: multiple states and proton transfer. *Proc Natl Acad Sci U S A* 93: 8362–8367, 1996.
21. Chavez V, Mohri-Shiomi A, and Garsin DA. Ce-Duox1/BLI-3 generates reactive oxygen species as a protective innate immune mechanism in *Caenorhabditis elegans*. *Infect Immun* 77: 4983–4989, 2009.
22. Chavez V, Mohri-Shiomi A, Maadani A, Vega LA, and Garsin DA. Oxidative stress enzymes are required for DAF-16-mediated immunity due to generation of reactive oxygen species by *Caenorhabditis elegans*. *Genetics* 176: 1567–1577, 2007.
23. Cheng H, Wang W, Wang X, Sheu SS, Dirksen RT, and Dong MQ. Cheng *et al.* reply. *Nature* 514: E14–E15, 2014.
24. Coburn C and Gems D. The mysterious case of the *C. elegans* gut granule: death fluorescence, anthranilic acid and the kynurenine pathway. *Front Genet* 4: 151, 2013.
25. Cocheme HM, Quin C, McQuaker SJ, Cabreiro F, Logan A, Prime TA, Abakumova I, Patel JV, Fearnley IM, James AM, Porteous CM, Smith RA, Saeed S, Carre JE, Singer M, Gems D, Hartley RC, Partridge L, and Murphy MP. Measurement of H2O2 within living *Drosophila* during aging using a ratiometric mass spectrometry probe targeted to the mitochondrial matrix. *Cell Metab* 13: 340–350, 2011.
26. De Haes W, Frooninckx L, Van Assche R, Smolders A, Depuydt G, Billen J, Braeckman BP, Schoofs L, and Temmerman L. Metformin promotes lifespan through mitohormesis via the peroxiredoxin PRDX-2. *Proc Natl Acad Sci U S A* 111: E2501–E2509, 2014.
27. De Henau S, Tilleman L, Vangheel M, Luyckx E, Trashin S, Pauwels M, Germani F, Vlaeminck C, Vanfleteren JR, Bert W, Pesce A, Nardini M, Bolognesi M, De Wael K, Moens L, Dewilde S, and Braeckman BP. A redox signalling globin is essential for reproduction in *Caenorhabditis elegans*. *Nat Commun* 6: 8782, 2015.
28. Dickinson BC and Chang CJ. Chemistry and biology of reactive oxygen species in signaling or stress responses. *Nat Chem Biol* 7: 504–511, 2011.
29. Dickinson BC, Tang Y, Chang Z, and Chang CJ. A nuclear-localized fluorescent hydrogen peroxide probe for monitoring sirtuin-mediated oxidative stress responses in vivo. *Chem Biol* 18: 943–948, 2011.
30. Dooley CT, Dore TM, Hanson GT, Jackson WC, Remington SJ, and Tsien RY. Imaging dynamic redox changes in mammalian cells with green fluorescent protein indicators. *J Biol Chem* 279: 22284–22293, 2004.
31. Doonan R, McElwee JJ, Matthijssens F, Walker GA, Houthoofd K, Back P, Matscheski A, Vanfleteren JR, and Gems D. Against the oxidative damage theory of aging: superoxide dismutases protect against oxidative stress but have little or no effect on life span in *Caenorhabditis elegans*. *Genes Dev* 22: 3236–3241, 2008.
32. Droge W. Oxidative stress and aging. *Adv Exp Med Biol* 543: 191–200, 2003.
33. Edens WA, Sharling L, Cheng G, Shapira R, Kinkade JM, Lee T, Edens HA, Tang X, Sullards C, Flaherty DB, Benian GM, and Lambeth JD. Tyrosine cross-linking of extracellular matrix is catalyzed by Duox, a multidomain oxidase/peroxidase with homology to the phagocyte oxidase subunit gp91phox. *J Cell Biol* 154: 879–891, 2001.
34. Ermakova YG, Bilan DS, Matlashov ME, Mishina NM, Markvicheva KN, Subach OM, Subach FV, Bogeski I, Hoth M, Enikolopov G, and Belousov VV. Red fluorescent genetically encoded indicator for intracellular hydrogen peroxide. *Nat Commun* 5: 5222, 2014.
35. Evans TC. Transformation and microinjection. In: *WormBook*, edited by Community TCeR, 2006.
36. Fierro-Gonzalez JC, Cornils A, Alcedo J, Miranda-Vizuete A, and Swoboda P. The thioredoxin TRX-1 modulates the function of the insulin-like neuropeptide DAF-28 during dauer formation in *Caenorhabditis elegans*. *PLoS One* 6: e16561, 2011.
37. Fierro-Gonzalez JC, Gonzalez-Barrios M, Miranda-Vizuete A, and Swoboda P. The thioredoxin TRX-1 regulates adult lifespan extension induced by dietary restriction in *Caenorhabditis elegans*. *Biochem Biophys Res Commun* 406: 478–482, 2011.
38. Fisher AB. Redox signaling across cell membranes. *Antioxid Redox Signal* 11: 1349–1356, 2009.
39. Fricker MD. Quantitative redox imaging software. *Antioxid Redox Signal* 24: 752–762 2015.
40. Frokjaer-Jensen C. Exciting prospects for precise engineering of *Caenorhabditis elegans* genomes with CRISPR/Cas9. *Genetics* 195: 635–642, 2013.
41. Frokjaer-Jensen C, Davis MW, Hopkins CE, Newman BJ, Thummel JM, Olesen SP, Grunnet M, and Jorgensen EM. Single-copy insertion of transgenes in *Caenorhabditis elegans*. *Nat Genet* 40: 1375–1383, 2008.

42. Fu X, Tang Y, Dickinson BC, Chang CJ, and Chang Z. An oxidative fluctuation hypothesis of aging generated by imaging H(2)O(2) levels in live *Caenorhabditis elegans* with altered lifespans. *Biochem Biophys Res Commun* 458: 896–900, 2015.
43. Fujii M, Ishii N, Joguchi A, Yasuda K, and Ayusawa D. A novel superoxide dismutase gene encoding membrane-bound and extracellular isoforms by alternative splicing in *Caenorhabditis elegans*. *DNA Res* 5: 25–30, 1998.
44. Ghose P, Park EC, Tabakin A, Salazar-Vasquez N, and Rongo C. Anoxia-reoxygenation regulates mitochondrial dynamics through the hypoxia response pathway, SKN-1/Nrf, and stomatin-like protein STL-1/SLP-2. *PLoS Genet* 9: e1004063, 2013.
45. Gomes A, Fernandes E, and Lima JL. Fluorescence probes used for detection of reactive oxygen species. *J Biochem Biophys Methods* 65: 45–80, 2005.
46. Gotoh O. Divergent structures of *Caenorhabditis elegans* cytochrome P450 genes suggest the frequent loss and gain of introns during the evolution of nematodes. *Mol Biol Evol* 15: 1447–1459, 1998.
47. Green RA, Audhya A, Pozniakovsky A, Dammermann A, Pemble H, Monen J, Portier N, Hyman A, Desai A, and Oegema K. Expression and imaging of fluorescent proteins in the *C. elegans* gonad and early embryo. *Methods Cell Biol* 85: 179–218, 2008.
48. Gutscher M, Pauleau AL, Marty L, Brach T, Wabnitz GH, Samstag Y, Meyer AJ, and Dick TP. Real-time imaging of the intracellular glutathione redox potential. *Nat Methods* 5: 553–559, 2008.
49. Gutscher M, Sobotta MC, Wabnitz GH, Ballikaya S, Meyer AJ, Samstag Y, and Dick TP. Proximity-based protein thiol oxidation by H_2O_2-scavenging peroxidases. *J Biol Chem* 284: 31532–31540, 2009.
50. Hall DH, Winfrey VP, Blaeuer G, Hoffman LH, Furuta T, Rose KL, Hobert O, and Greenstein D. Ultrastructural features of the adult hermaphrodite gonad of *Caenorhabditis elegans*: relations between the germ line and soma. *Dev Biol* 212: 101–123, 1999.
51. Halliwell B and Gutteridge J. *Free Radicals in Biology and Medicine*, 4th edn. Oxford: Oxford University Press, 2007.
52. Hitchler MJ and Domann FE. An epigenetic perspective on the free radical theory of development. *Free Radic Biol Med* 43: 1023–1036, 2007.
53. Hoeven R, McCallum KC, Cruz MR, and Garsin DA. Ce-Duox1/BLI-3 generated reactive oxygen species trigger protective SKN-1 activity via p38 MAPK signaling during infection in *C. elegans*. *PLoS Pathog* 7: e1002453, 2011.
54. Honda Y, Tanaka M, and Honda S. Modulation of longevity and diapause by redox regulation mechanisms under the insulin-like signaling control in *Caenorhabditis elegans*. *Exp Gerontol* 43: 520–529, 2008.
55. Hoogewijs D, Geuens E, Dewilde S, Vierstraete A, Moens L, Vinogradov S, and Vanfleteren JR. Wide diversity in structure and expression profiles among members of the *Caenorhabditis elegans* globin protein family. *BMC Genomics* 8: 356, 2007.
56. Hoogewijs D, Houthoofd K, Matthijssens F, Vandesompele J, and Vanfleteren JR. Selection and validation of a set of reliable reference genes for quantitative sod gene expression analysis in *C. elegans*. *BMC Mol Biol* 9: 9, 2008.
57. Huang Z, Zhang W, Fang H, Zheng M, Wang X, Xu J, Cheng H, Gong G, Wang W, Dirksen RT, and Sheu SS. Response to ''A critical evaluation of cpYFP as a probe for superoxide''. *Free Radic Biol Med* 51: 1937–1940, 2011.
58. Husson SJ, Mertens I, Janssen T, Lindemans M, and Schoofs L. Neuropeptidergic signaling in the nematode *Caenorhabditis elegans*. *Prog Neurobiol* 82: 33–55, 2007.
59. Isermann K, Liebau E, Roeder T, and Bruchhaus I. A peroxiredoxin specifically expressed in two types of pharyngeal neurons is required for normal growth and egg production in *Caenorhabditis elegans*. *J Mol Biol* 338: 745–755, 2004.
60. Jackson MJ. Reactive oxygen species and redox-regulation of skeletal muscle adaptations to exercise. *Philos Trans R Soc Lond B Biol Sci* 360: 2285–2291, 2005.
61. Jee C, Vanoaica L, Lee J, Park BJ, and Ahnn J. Thioredoxin is related to life span regulation and oxidative stress response in *Caenorhabditis elegans*. *Genes Cells* 10: 1203–1210, 2005.
62. Jensen LT and Culotta VC. Activation of CuZn superoxide dismutases from *Caenorhabditis elegans* does not require the copper chaperone CCS. *J Biol Chem* 280: 41373–41379, 2005.
63. Johnson D and Nehrke K. Mitochondrial fragmentation leads to intracellular acidification in *Caenorhabditis elegans* and mammalian cells. *Mol Biol Cell* 21: 2191–2201, 2010.
64. Kaludercic N, Deshwal S, and Di Lisa F. Reactive oxygen species and redox compartmentalization. *Front Physiol* 5: 285, 2014.
65. Kawasaki I, Hanazawa M, Gengyo-Ando K, Mitani S, Maruyama I, and Iino Y. ASB-1, a germline-specific isoform of mitochondrial ATP synthase b subunit, is required to maintain the rate of germline development in *Caenorhabditis elegans*. *Mech Dev* 124: 237–251, 2007.
66. Kim E, Sun L, Gabel CV, and Fang-Yen C. Long-term imaging of *Caenorhabditis elegans* using nanoparticle-mediated immobilization. *PLoS One* 8: e53419, 2013.
67. Kimble J and Crittenden SL. Controls of germline stem cells, entry into meiosis, and the sperm/oocyte decision in *Caenorhabditis elegans*. *Annu Rev Cell Dev Biol* 23: 405–433, 2007.
68. Kirstein J, Morito D, Kakihana T, Sugihara M, Minnen A, Hipp MS, Nussbaum-Krammer C, Kasturi P, Hartl FU, Nagata K, and Morimoto RI. Proteotoxic stress and ageing triggers the loss of redox homeostasis across cellular compartments. *EMBO J* 34: 2334–2349, 2015.
69. Knoefler D, Thamsen M, Koniczek M, Niemuth NJ, Diederich AK, and Jakob U. Quantitative in vivo redox sensors uncover oxidative stress as an early event in life. *Mol Cell* 47: 767–776, 2012.
70. Kubagawa HM, Watts JL, Corrigan C, Edmonds JW, Sztul E, Browse J, and Miller MA. Oocyte signals derived from polyunsaturated fatty acids control sperm recruitment in vivo. *Nat Cell Biol* 8: 1143–1148, 2006.
71. Kumsta C, Thamsen M, and Jakob U. Effects of oxidative stress on behavior, physiology, and the redox thiol proteome of *Caenorhabditis elegans*. *Antioxid Redox Signal* 14: 1023–1037, 2011.
72. Lee SJ, Hwang AB, and Kenyon C. Inhibition of respiration extends *C. elegans* life span via reactive oxygen species that increase HIF-1 activity. *Curr Biol* 20: 2131–2136, 2010.
73. Leiers B, Kampkotter A, Grevelding CG, Link CD, Johnson TE, and Henkle-Duhrsen K. A stress-responsive glutathione S-transferase confers resistance to oxidative stress in *Caenorhabditis elegans*. *Free Radic Biol Med* 34: 1405–1415, 2003.

74. Levin M, Hashimshony T, Wagner F, and Yanai I. Developmental milestones punctuate gene expression in the *Caenorhabditis* embryo. *Dev Cell* 22: 1101–1108, 2012.
75. Li X, Johnson RW, Park D, Chin-Sang I, and Chamberlin HM. Somatic gonad sheath cells and Eph receptor signaling promote germ-cell death in *C. elegans*. *Cell Death Differ* 19: 1080–1089, 2012.
76. Link CD and Johnson CJ. Reporter transgenes for study of oxidant stress in *Caenorhabditis elegans*. *Methods Enzymol* 353: 497–505, 2002.
77. Lukyanov KA and Belousov VV. Genetically encoded fluorescent redox sensors. *Biochim Biophys Acta* 1840: 745–756, 2014.
78. Malinouski M, Zhou Y, Belousov VV, Hatfield DL, and Gladyshev VN. Hydrogen peroxide probes directed to different cellular compartments. *PLoS One* 6: e14564, 2011.
79. Marfori M, Mynott A, Ellis JJ, Mehdi AM, Saunders NF, Curmi PM, Forwood JK, Boden M, and Kobe B. Molecular basis for specificity of nuclear import and prediction of nuclear localization. *Biochim Biophys Acta* 1813: 1562–1577, 2010.
80. Mariol MC, Walter L, Bellemin S, and Gieseler K. A rapid protocol for integrating extrachromosomal arrays with high transmission rate into the *C. elegans* genome. *J Vis Exp* e50773, 2013.
81. Markvicheva KN, Bilan DS, Mishina NM, Gorokhovatsky AY, Vinokurov LM, Lukyanov S, and Belousov VV. A genetically encoded sensor for H_2O_2 with expanded dynamic range. *Bioorg Med Chem* 19: 1079–1084, 2011.
82. McCarter J, Bartlett B, Dang T, and Schedl T. Soma-germ cell interactions in *Caenorhabditis elegans*: multiple events of hermaphrodite germline development require the somatic sheath and spermathecal lineages. *Dev Biol* 181: 121–143, 1997.
83. Merritt C, Rasoloson D, Koa D, and Seydoux G. 3′ UTRs are the primary regulators of gene expression in the *C. elegans* germline. *Curr Biol* 18: 1476–1482, 2008.
84. Meyer AJ and Dick TP. Fluorescent protein-based redox probes. *Antioxid Redox Signal* 13: 621–650, 2010.
85. Miranda-Vizuete A, Fierro Gonzalez JC, Gahmon G, Burghoorn J, Navas P, and Swoboda P. Lifespan decrease in a *Caenorhabditis elegans* mutant lacking TRX-1, a thioredoxin expressed in ASJ sensory neurons. *FEBS Lett* 580: 484–490, 2006.
86. Mishina NM, Tyurin-Kuzmin PA, Markvicheva KN, Vorotnikov AV, Tkachuk VA, Laketa V, Schultz C, Lukyanov S, and Belousov VV. Does cellular hydrogen peroxide diffuse or act locally? *Antioxid Redox Signal* 14: 1–7, 2011.
87. Morgan B, Sobotta MC, and Dick TP. Measuring E(GSH) and H_2O_2 with roGFP2-based redox probes. *Free Radic Biol Med* 51: 1943–1951, 2011.
88. Muller FL. A critical evaluation of cpYFP as a probe for superoxide. *Free Radic Biol Med* 47: 1779–1780, 2009.
89. Olahova M, Taylor SR, Khazaipoul S, Wang J, Morgan BA, Matsumoto K, Blackwell TK, and Veal EA. A redox-sensitive peroxiredoxin that is important for longevity has tissue- and stress-specific roles in stress resistance. *Proc Natl Acad Sci U S A* 105: 19839–19844, 2008.
90. Olahova M and Veal EA. A peroxiredoxin, PRDX-2, is required for insulin secretion and insulin/IIS-dependent regulation of stress resistance and longevity. *Aging Cell* 14: 558–568, 2015.
91. Ostergaard H, Henriksen A, Hansen FG, and Winther JR. Shedding light on disulfide bond formation: engineering a redox switch in green fluorescent protein. *EMBO J* 20: 5853–5862, 2001.
92. Petriv OI and Rachubinski RA. Lack of peroxisomal catalase causes a progeric phenotype in *Caenorhabditis elegans*. *J Biol Chem* 279: 19996–20001, 2004.
93. Pierce SB, Costa M, Wisotzkey R, Devadhar S, Homburger SA, Buchman AR, Ferguson KC, Heller J, Platt DM, Pasquinelli AA, Liu LX, Doberstein SK, and Ruvkun G. Regulation of DAF-2 receptor signaling by human insulin and ins-1, a member of the unusually large and diverse *C. elegans* insulin gene family. *Genes Dev* 15: 672–686, 2001.
94. Praitis V, Casey E, Collar D, and Austin J. Creation of low-copy integrated transgenic lines in *Caenorhabditis elegans*. *Genetics* 157: 1217–1226, 2001.
95. Prevedel R, Yoon YG, Hoffmann M, Pak N, Wetzstein G, Kato S, Schrodel T, Raskar R, Zimmer M, Boyden ES, and Vaziri A. Simultaneous whole-animal 3D imaging of neuronal activity using light-field microscopy. *Nat Methods* 11: 727–730, 2014.
96. Putker M, Madl T, Vos HR, de Ruiter H, Visscher M, van den Berg MC, Kaplan M, Korswagen HC, Boelens R, Vermeulen M, Burgering BM, and Dansen TB. Redox-dependent control of FOXO/DAF-16 by transportin-1. *Mol Cell* 49: 730–742, 2013.
97. Quatresous E, Legrand C, and Pouvreau S. Mitochondria-targeted cpYFP: pH or superoxide sensor? *J Gen Physiol* 140: 567–570, 2012.
98. Rea SL, Ventura N, and Johnson TE. Relationship between mitochondrial electron transport chain dysfunction, development, and life extension in *Caenorhabditis elegans*. *PLoS Biol* 5: e259, 2007.
99. Redemann S, Schloissnig S, Ernst S, Pozniakowsky A, Ayloo S, Hyman AA, and Bringmann H. Codon adaptation-based control of protein expression in *C. elegans*. *Nat Methods* 8: 250–252, 2011.
100. Rogers JM and Hunter ES, 3rd. Redox redux: a closer look at conceptal low molecular weight thiols. *Toxicol Sci* 62: 1–3, 2001.
101. Romero-Aristizabal C, Marks DS, Fontana W, and Apfeld J. Regulated spatial organization and sensitivity of cytosolic protein oxidation in *Caenorhabditis elegans*. *Nat Commun* 5: 5020, 2014.
102. San-Miguel A and Lu H. Microfluidics as a tool for *C. elegans* research. *WormBook* 24: 1–19, 2013.
103. Santo-Domingo J, Giacomello M, Poburko D, Scorrano L, and Demaurex N. OPA1 promotes pH flashes that spread between contiguous mitochondria without matrix protein exchange. *EMBO J* 32: 1927–1940, 2013.
104. Schaar CE, Dues DJ, Spielbauer KK, Machiela E, Cooper JF, Senchuk M, Hekimi S, and Van Raamsdonk JM. Mitochondrial and cytoplasmic ROS have opposing effects on lifespan. *PLoS Genet* 11: e1004972, 2015.
105. Schafer FQ and Buettner GR. Redox environment of the cell as viewed through the redox state of the glutathione disulfide/glutathione couple. *Free Radic Biol Med* 30: 1191–1212, 2001.
106. Schmeisser S, Priebe S, Groth M, Monajembashi S, Hemmerich P, Guthke R, Platzer M, and Ristow M. Neuronal ROS signaling rather than AMPK/sirtuin-mediated energy sensing links dietary restriction to lifespan extension. *Mol Metab* 2: 92–102, 2013.
107. Schwarzlander M, Dick TP, Meye AJ, and Morgan B. Dissecting redox biology using fluorescent protein sensors. *Antioxid Redox Signal* 24: 680–712, 2016.

108. Schwarzlander M, Fricker MD, Muller C, Marty L, Brach T, Novak J, Sweetlove LJ, Hell R, and Meyer AJ. Confocal imaging of glutathione redox potential in living plant cells. *J Microsc* 231: 299–316, 2008.
109. Schwarzlander M, Wagner S, Ermakova YG, Belousov VV, Radi R, Beckman JS, Buettner GR, Demaurex N, Duchen MR, Forman HJ, Fricker MD, Gems D, Halestrap AP, Halliwell B, Jakob U, Johnston IG, Jones NS, Logan DC, Morgan B, Muller FL, Nicholls DG, Remington SJ, Schumacker PT, Winterbourn CC, Sweetlove LJ, Meyer AJ, Dick TP, and Murphy MP. The 'mitoflash' probe cpYFP does not respond to superoxide. *Nature* 514: E12–E14, 2014.
110. Shaham S. Methods in cell biology. *WormBook* 13: 1–75, 2006.
111. Shen EZ, Song CQ, Lin Y, Zhang WH, Su PF, Liu WY, Zhang P, Xu J, Lin N, Zhan C, Wang X, Shyr Y, Cheng H, and Dong MQ. Mitoflash frequency in early adulthood predicts lifespan in *Caenorhabditis elegans*. *Nature* 508: 128–132, 2014.
112. Shibata Y, Branicky R, Landaverde IO, and Hekimi S. Redox regulation of germline and vulval development in *Caenorhabditis elegans. Science* 302: 1779–1782, 2003.
113. Srikun D, Albers AE, Nam CI, Iavarone AT, and Chang CJ. Organelle-targetable fluorescent probes for imaging hydrogen peroxide in living cells via SNAP-Tag protein labeling. *J Am Chem Soc* 132: 4455–4465, 2010.
114. Stein L, Sternberg P, Durbin R, Thierry-Mieg J, and Spieth J. WormBase: network access to the genome and biology of *Caenorhabditis elegans*. *Nucleic Acids Res* 29: 82–86, 2001.
115. Stenvall J, Fierro-Gonzalez JC, Swoboda P, Saamarthy K, Cheng Q, Cacho-Valadez B, Arner ES, Persson OP, Miranda-Vizuete A, and Tuck S. Selenoprotein TRXR-1 and GSR-1 are essential for removal of old cuticle during molting in *Caenorhabditis elegans*. *Proc Natl Acad Sci U S A* 108: 1064–1069, 2011.
116. Stiernagle T. Maintenance of *C. elegans*. *WormBook* 11: 1–19, 2013.
117. Stinchcomb DT, Shaw JE, Carr SH, and Hirsh D. Extrachromosomal DNA transformation of *Caenorhabditis elegans*. *Mol Cell Biol* 5: 3484–3496, 1985.
118. Sulston JE and Horvitz HR. Post-embryonic cell lineages of the nematode, *Caenorhabditis elegans*. *Dev Biol* 56: 110–156, 1977.
119. Suthammarak W, Somerlot BH, Opheim E, Sedensky M, and Morgan PG. Novel interactions between mitochondrial superoxide dismutases and the electron transport chain. *Aging Cell* 12: 1132–1140, 2013.
120. Tabara H, Sarkissian M, Kelly WG, Fleenor J, Grishok A, Timmons L, Fire A, and Mello CC. The rde-1 gene, RNA interference, and transposon silencing in *C. elegans*. *Cell* 99: 123–132, 1999.
121. Tang L and Choe KP. Characterization of skn-1/wdr-23 phenotypes in *Caenorhabditis elegans*; pleiotrophy, aging, glutathione, and interactions with other longevity pathways. *Mech Ageing Dev* 149: 88–98, 2015.
122. Tantama M, Hung YP, and Yellen G. Imaging intracellular pH in live cells with a genetically encoded red fluorescent protein sensor. *J Am Chem Soc* 133: 10034–10037, 2011.
123. Timmons L, Court DL, and Fire A. Ingestion of bacterially expressed dsRNAs can produce specific and potent genetic interference in *Caenorhabditis elegans*. *Gene* 263: 103–112, 2001.
124. Togo SH, Maebuchi M, Yokota S, Bun-Ya M, Kawahara A, and Kamiryo T. Immunological detection of alkaline-diaminobenzidine-negativeperoxisomes of the nematode *Caenorhabditis elegans* purification and unique pH optima of peroxisomal catalase. *Eur J Biochem* 267: 1307–1312, 2000.
125. Van Raamsdonk JM and Hekimi S. Superoxide dismutase is dispensable for normal animal lifespan. *Proc Natl Acad Sci U S A* 109: 5785–5790, 2012.
126. Wang H, Karadge U, Humphries WH, 4th, and Fisher AL. Analyzing cell physiology in *C. elegans* with fluorescent ratiometric reporters. *Methods* 68: 508–517, 2014.
127. Wang W, Fang H, Groom L, Cheng A, Zhang W, Liu J, Wang X, Li K, Han P, Zheng M, Yin J, Mattson MP, Kao JP, Lakatta EG, Sheu SS, Ouyang K, Chen J, Dirksen RT, and Cheng H. Superoxide flashes in single mitochondria. *Cell* 134: 279–290, 2008.
128. Wang Y, Ezemaduka AN, Tang Y, and Chang Z. Understanding the mechanism of the dormant dauer formation of *C. elegans*: from genetics to biochemistry. *IUBMB Life* 61: 607–612, 2009.
129. Wardman P. Fluorescent and luminescent probes for measurement of oxidative and nitrosative species in cells and tissues: progress, pitfalls, and prospects. *Free Radic Biol Med* 43: 995–1022, 2007.
130. White JG, Southgate E, Thomson JN, and Brenner S. The structure of the nervous system of the nematode *Caenorhabditis elegans*. *Philos Trans R Soc Lond B Biol Sci* 314: 1–340, 1986.
131. Woollard A. Gene duplications and genetic redundancy in *C. elegans. WormBook* 1–6, 2005.
132. Xu S and Chisholm AD. *C. elegans* epidermal wounding induces a mitochondrial ROS burst that promotes wound repair. *Dev Cell* 31: 48–60, 2014.
133. Yanase S, Onodera A, Tedesco P, Johnson TE, and Ishii N. SOD-1 deletions in *Caenorhabditis elegans* alter the localization of intracellular reactive oxygen species and show molecular compensation. *J Gerontol A Biol Sci Med Sci* 64: 530–539, 2009.
134. Yang W and Hekimi S. A mitochondrial superoxide signal triggers increased longevity in *Caenorhabditis elegans*. *PLoS Biol* 8: e1000556, 2010.
135. Yang Y, Han SM, and Miller MA. MSP hormonal control of the oocyte MAP kinase cascade and reactive oxygen species signaling. *Dev Biol* 342: 96–107, 2010.
136. Yee C, Yang W, and Hekimi S. The intrinsic apoptosis pathway mediates the pro-longevity response to mitochondrial ROS in *C. elegans*. *Cell* 157: 897–909, 2014.
137. Yoon J, Herzik MA, Jr., Winter MB, Tran R, Olea C, Jr., and Marletta MA. Structure and properties of a bis-histidyl ligated globin from *Caenorhabditis elegans*. *Biochemistry* 49: 5662–5670, 2010.

Address correspondence to:
Prof. Bart P. Braeckman
Biology Department
Ghent University
Proeftuinstraat 86 N1
Ghent 9000
Belgium

E-mail: bart.braeckman@ugent.be

Date of first submission to ARS Central, May 26, 2016; date of acceptance, June 14, 2016.

Abbreviations Used

4D = four dimensional
CAN neuron = canal-associated neuron
cpYFP = circularly permuted yellow fluorescent protein
CRISPR/Cas9 = clustered regularly interspaced short palindromic repeats/CRISPR-associated CrRNA 9
CTL = catalase
DTT = dithiothreitol
eGFP = enhanced green fluorescent protein
ER = endoplasmic reticulum
GFP = green fluorescent protein
GSH = reduced glutathione
GSSG = oxidized glutathione dimer
GST = glutathione-*S*-transferase
H_2O_2 = hydrogen peroxide
HyPer = hydrogen peroxide sensor
IGF = insulin-like growth factor
INR = intensity-normalized ratio
L4 = fourth larval stage
MLS = mitochondrial localization sequence
MosSCI = mos1-mediated single copy insertion
PQ = paraquat
RNAi = RNA interference
roGFP = reduction–oxidation-sensitive green fluorescent protein
ROS = reactive oxygen species
rxYFP = redox-sensitive yellow fluorescent protein
SOD = superoxide dismutase
UV = ultraviolet
YFP = yellow fluorescent protein